Available online at www.sciencedirect.com
SCIENCE DIRECT®
Journal of Solid State Chemistry 178 (2005) 435–440
JOURNAL OF SOLID STATE CHEMISTRY
www.elsevier.com/locate/jssc

A few remarks on the simulation and use of crystal field energy level schemes of the rare earth ions

Jorma Hölsä[a], Mika Lastusaari[a,*], Miroslav Maryško[b], Mika Tukia[a]

[a]*Laboratory of Inorganic Chemistry, Department of Chemistry, University of Turku, FI-20014 Turku, Finland*
[b]*Institute of Physics, The Academy of Sciences of the Czech Republic, Cukrovarnická 10, CZ-162 53 Praha 6, Czech Republic*

Received 19 May 2004; received in revised form 13 August 2004; accepted 7 September 2004
Available online 11 November 2004

Abstract

The usefulness of the simulation of the energy level schemes of the trivalent rare earth (R^{3+}) ions in the prediction of the properties of the rare earth compounds is demonstrated for a few selected cases emphasizing the connection between different spectroscopic and magnetic properties of the R^{3+} ions. The importance of the calculated energy level schemes in the UV-VUV range in interpreting complicated spectra and designing new phosphors by energy transfer and quantum cutting is described. In the absence of direct measurements, the calculated energy level values can be very useful. The possibilities to interpret the magnetic properties of the R^{3+} (and R^{2+}) ions are described by using the wave functions of the energy levels obtained from the energy level simulations. As a fine example, it is shown how the amount of an Eu^{2+} impurity can be obtained from the calculation of the paramagnetic susceptibility as a function of temperature. The problems involved in the simulation of the ^7F_J crystal field energy level scheme of the Eu^{3+} ion are highlighted by using a comparison between the extensive literature data and calculated level schemes.

Keywords: Rare earth; Energy level scheme; Paramagnetic susceptibility; Europium

1. Introduction

The $4f^N$ energy level structures of the rare earth (R) ions and the interactions behind these have been subject to intense investigations since the early 1950s [1]. Several books of great value have been written upon the results of these analyses [2–5]. At the moment, it may seem that not much is left to do. However, this is only a delusion since the ideas take a long time to be realized. For instance, the quantum cutting, i.e., achievement of higher than 100 percent quantum efficiency was already presented as an idea in the 1950s but the experimental proof of this phenomenon came to light only in the early 1990s. To be frank, this two to three hundred percent quantum efficiency does not imply that the energy efficiency should be very different from that in ordinary luminescence since there are considerable energy losses with the VUV excitation.

Another example of a very recent and highly interesting subject is the rare earth-doped compound, which shows the phenomenon called persistent luminescence [6]. This phenomenon has always been looked upon unfavorably by every phosphor company engineer and scientist. Indeed, the afterglow has destroyed many a good phosphor material, as the fate of the alkali metal aluminates doped with divalent europium shows: these excellent luminescence materials were left in oblivescence from the mid-1960s to 1990s but since then they have arisen from the shadows into the frame lights as efficient persistent luminescence materials.

There are several other examples where the exact knowledge of the $4f^N$ energy level structure may initially be of great importance if new phenomena were to be

*Corresponding author. Fax: +358 2 333 6700.
E-mail address: miklas@utu.fi (M. Lastusaari).

0022-4596/$ - see front matter © 2004 Elsevier Inc. All rights reserved.
doi:10.1016/j.jssc.2004.09.027

realized and exploited. In this paper, the authors want to honor the work of one of the early pioneers, Dr. W.T. Carnall, in the field of rare earth (and actinide) spectroscopy and energy level simulation. Some 42 years after his first scientific paper on the spectroscopic properties of lanthanides [7], the work started by him is still of great value and more importantly, becoming more reliable. It must be remembered that, at the moment, the ab initio calculations do not give any reliable values even for the $^{2S+1}L_J$ level structure. The semi-empirical simulation of the experimental energy level schemes is much more reliable and the results are of practical use though the work involved is usually very tedious. Accordingly, the results of the energy level simulations should always be considered with some care since there exist several pitfalls in the procedures, e.g., the least-squares refinements generally used.

2. Energy level scheme calculations

The complex energy level schemes of the R^{3+} ions in solid state result from several interactions—both within the $4f^N$ electron configuration and between the R^{3+} ion and its environment [4]. Each interaction can be described with the aid of effective operators and, consequently, their effect can be parameterized by using phenomenological models. The Coulombic interaction between the $4f$ electrons is described with the Slater integrals F^k ($k = 0$, 2, 4, and 6) or Racah parameters E_k ($k = 0$, 1, 2, and 3). The spin–orbit coupling taken into account by a sole coupling constant (ζ_{4f}) splits the ^{2S+1}L terms into the $^{2S+1}L_J$ levels. α, β and γ describe the two-body electrostatic Trees parameters, whereas the Judd parameters T^k ($k = 2, 3, 4, 6, 7, 8$) are the corresponding three-body interactions. The effective free ion Hamiltonian H_{FI} comprising these interactions can be written as follows:

$$H_{\mathrm{FI}} = \sum_{k=0}^{3} E_k(nf, nf)e^k + \zeta_{4f}A_{\mathrm{SO}} + \alpha L(L+1) + \beta G(G_2) + \gamma G(R_7) + \sum_{k=2,3,4,6,7,8} T^k t_k, \quad (1)$$

where the angular parts, $e^k, A_{\mathrm{SO}}, L, G(G_2), G(R_7)$, and t_k, have their usual meanings [4,8]. Higher-order magnetic spin–spin and spin–other orbit interactions as well as the electrostatically correlated spin–orbit interactions can be parameterized by the Marvin integrals M^k ($k = 0$, 2, and 4) and P^k ($k = 2$, 4, and 6), respectively.

When the R^{3+} ion is introduced into a solid it experiences an inhomogeneous electrostatic field created by the surrounding charge distribution originating from the ligands. The crystal field (c.f.) Hamiltonian H_{CF} describing the effect of this field can be written as follows [4]:

$$H_{\mathrm{CF}} = \sum_k \sum_{q=-k}^{q=k} \left\{ B_q^k \left[C_q^k + (-1)^q C_{-q}^k \right] + \mathrm{i}S_q^k \left[C_q^k - (-1)^{-q} C_{-q}^k \right] \right\}, \quad (2)$$

where the c.f. parameters B_q^k and S_q^k are the coefficients of the c.f. expansion, i.e., the real and imaginary functions of the radial distances, respectively. The C_q^k's are tensor operators of rank k (with $q \leqslant k$) closely related to spherical harmonics. In addition to the one-electron c.f. contribution, several works have considered two-electron contributions and it has been found that, indeed, the c.f. splitting of some individual $^{2S+1}L_J$ levels were much better simulated than without the two-electron contributions [9,10]. The usefulness of these contributions is not clearly convincing since a rather high number of additional parameters must initially be considered—though not used.

2.1. About the reliability of the energy level simulations

Because of the well-protected nature of the $4f$ orbitals, the free ion parameters (Eq. (1)) do not vary much from one host to another [11] and, in the rare earth series, the evolution of these parameters should be smooth—even if one does not really know the values of all the parameters, e.g., the Marvin integrals. The smooth evolution of the free ion parameters was already shown by Carnall [8] tens of years ago in his works on the lanthanide trihalides. What is then the reality? Let us take the Eu^{3+} ion as an example since, of the R^{3+} ions, it is the most frequently used probe to investigate the spectra–structure relationship. Due to the simplicity of the c.f. splitting of the ^7F ground term and the relatively easy interpretation of the emission spectrum, the $^7F_{0-4}$ energy level scheme is simulated by using the experimental data readily obtained from the emission spectra. Assuming that the free ion effects have a negligible contribution to the $^7F_{JM}$ wave functions, the c.f. simulation can be carried out with the strongly reduced basis set of 49 $^7F_{0-6}$ levels. As a drawback of the severe truncation and the omission of the free ion effects, the experimental and simulated $^7F_{0-6}$ barycenters must be artificially adjusted to correspond to each other. In theory, the barycenter positions depend on only one free ion parameter, i.e., the spin–orbit coupling constant ζ_{4f} which should be the same for the whole $4f^6$ configuration comprising 3003 c.f. levels. Even more generally, the spin–orbit coupling constant seems to be rather independent of the host too.

How rigorously the artificial adjustment of the $^7F_{0-6}$ barycenters is done seems to depend mostly on the individual researcher (or a group) working on the subject. When the literature data comprising 132 sets

of *complete* experimental $^7F_{0-4}$ c.f. levels are analyzed, rather different c.f. energy level schemes are obtained which is not unusual owing to the different hosts compiled into the data set. On the other hand, one unique set of the $^7F_{0-4}$ barycenters (i.e., 0, 370, 1021, 1863, and 2829 cm^{-1}) was calculated by using the average free ion parameters [11] together with the spin–orbit coupling constant ζ_{4f} equal to 1332 cm^{-1}. Also the untruncated set of 3003 wave functions was then employed, and, more important, the c.f. effect was omitted by setting the B_q^k and S_q^k c.f. parameters equal to zero. When the experimental $^7F_{0-4}$ barycenter sets were plotted against the calculated one, significant differences could be observed (Fig. 1). First, the curves have different slopes which can readily be described as resulting from the slightly different spin–orbit coupling constant ζ_{4f} values. This deviation is of only limited interest though it may be a little surprising how close the slopes really are, i.e., the ζ_{4f} values are quite similar irrespective of the host lattice. The second observation is that the curves are not smooth linear plots. This is much more alarming since, according to preliminary full matrix calculations, all the experimental barycenters should fall on the same straight line, provided that the host is the same and the c.f. effect is omitted, of course.

It seems that, despite the evident simplicity of the 49 c.f. levels of the $^7F_{0-6}$ levels to be simulated, one should be very much aware of the possible pitfalls when the truncated sets of wave functions are used in the simulations. In the case of missing (or too many) experimental c.f. levels frequently resulting from the analysis of the emission spectra, the barycenters seem far too often to be misplaced. The misinterpretation of the positions of the c.f. levels leads, of course, to a wrong c.f. parameterization.

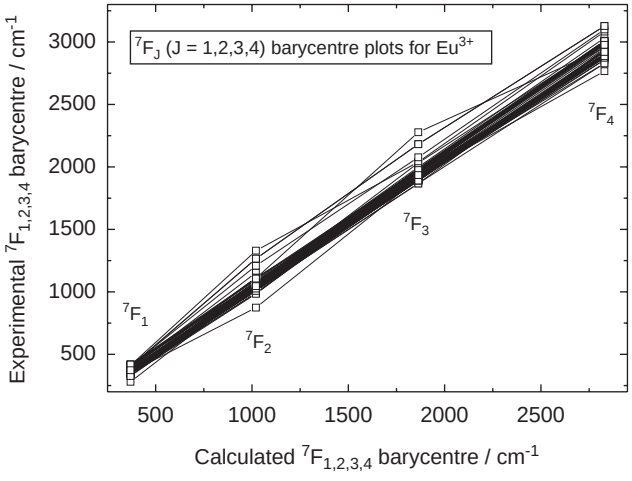

Fig. 1. Experimental barycenter values for the $^7F_{0-4}$ levels of 132 Eu^{3+} doped compounds as a function of the calculated free ion barycenters (without the crystal field effect).

In addition to the misinterpretation of the spectra, another solution to the deviation of the barycenter plots from a linear behavior may be suggested: in fact, the c.f. effect may have an influence on the $^7F_{0-6}$ barycenter positions. In order to establish these relationships, more work is needed, however. In the meanwhile, the fitting of the c.f. parameters to the c.f. energy level scheme of the ^7F ground term and analysis of the said schemes must be carried out with care and one should suppose that the barycenter curves as presented in Fig. 1 is linear. How this can be done is dealt with in the following.

The phenomenological simulation of the c.f. energy level schemes of the R^{3+} ions involves the derivation of a large number of parameters (even more than 30) [4] from the experimentally determined energy level scheme. The free ion parameters can be, a priori, obtained from any other simulation of the same R^{3+} electron configuration, or the average values can be used [11]. The same is not true with the c.f. parameters, the number of which may rise up to 15 for a low point symmetry case. Some schemes as the descending symmetry method as well as semi-empirical calculation of the c.f. parameters can be used to estimate the magnitude of some (or of a group of) c.f. parameters. In this case, there must, however, be a true connection between the actual and idealized crystal structure. In order to avoid the low symmetry problem, much debate and different approaches—both experimental and theoretical—have been taken in several studies. However, this problem has not been solved in a satisfactory manner to date. It is believed that the low symmetry problem will not be solved until the efficient multivariant algorithms are employed at the same level of sophistication as they are used in the simulated annealing and/or the genetic algorithms in solving the crystal structures from powder diffraction data.

3. Usefulness of energy level simulations

3.1. UV- and VUV levels: quantum cutting

In the introduction, it was stated that the idea of quantum cutting was already presented in the 1950s. However, in the early 1990s—some 40 years later—the practical means to realize this dream became available to the public (and to phosphor industry, as well). At the same time, the energy level simulations in the UV and VUV ranges were prevented in the past, by the inadequate experimental techniques to measure the levels of the $4f^N$ configuration and by the severe truncations used in the programs. The use of synchrotron facilities removed the first obstacle and the appearance of programs able to treat the whole $4f^N$ configuration as a basis set of wave functions seemed to remove the second obstacle. In such a way, the levels of

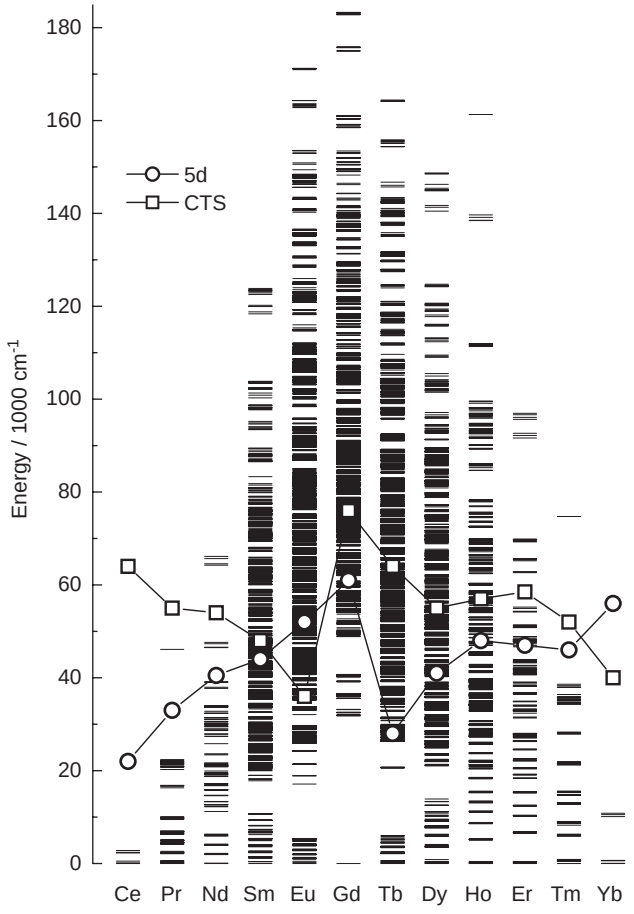

Fig. 2. Complete calculated energy level schemes for all and every R^{3+} ion from $4f^1$ (Ce^{3+}) to $4f^{13}$ (Yb^{3+}) in the ROBr host. The approximate positions of the lowest 5d levels and the charge transfer states are indicated with circles and squares, respectively.

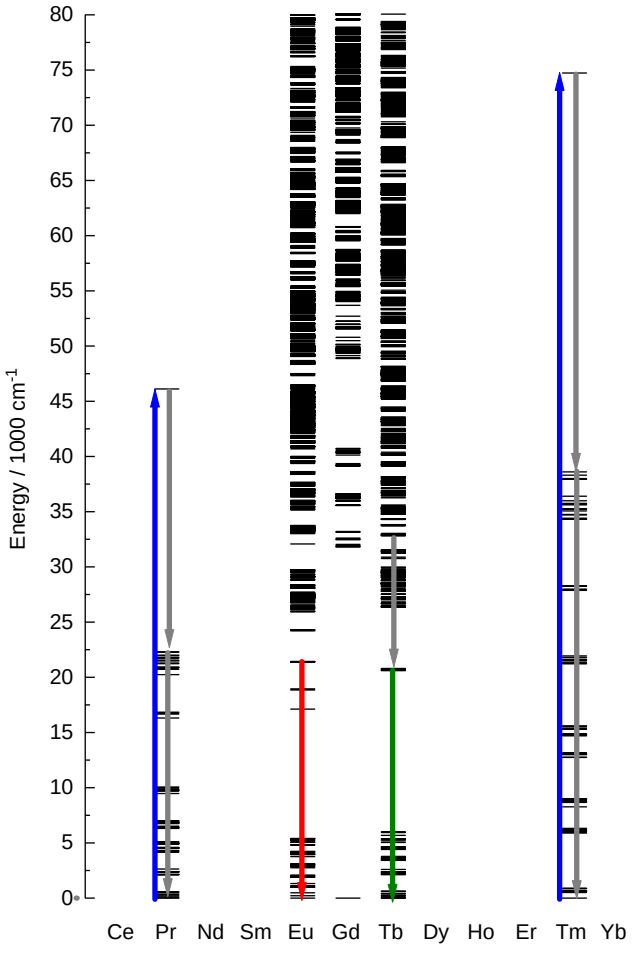

Fig. 3. Possible quantum cutting schemes for the Pr^{3+}, Eu^{3+}, Gd^{3+}, Tb^{3+} and Tm^{3+} ions.

the R^{3+} ions in the UV and VUV ranges could be calculated (Fig. 2) and the tailoring of the quantum cutting could start. For the Gd^{3+} ion, the higher energy levels could be determined and the proper visible red emission from Gd^{3+} due to the $^6G_J \rightarrow {}^6P_J$ transitions could be explained too [12,13]. When the Gd^{3+} ion is the sole dopant, emission of an ultraviolet photon due to the $^6P_J \rightarrow {}^8S_{7/2}$ transition follows the red (and NIR) emission. With the aid of energy transfer from Gd^{3+} to strongly emitting Eu^{3+} and Tb^{3+} ions introduced as co-dopants, the quantum efficiency of higher than one could be expected. However, the amount of energy wasted is still quite important and more elaborate systems should be designed.

Should this quantum cutting in the visible range work only with Gd^{3+}? There are two other ions, Pr^{3+} and Tm^{3+}, in the rare earth series, which present a large energy gap in their energy level scheme, both due to the isolated $^1S_0$ level at high energies (Fig. 3). For Pr^{3+}, the quantum cutting is not a new idea, whereas for the Tm^{3+} ion the experimental confirmation of this phenomenon is still lacking. The Tm^{3+} ion has the $^1S_0$ level with a calculated energy at 75000 cm^{-1} while the rest of the levels of the $4f^{12}$ configuration are at much lower energy, below 38000 cm^{-1}. The Tm^{3+} ion should thus be a possible candidate for quantum cutting though the lower $5d$ levels may severely interfere, maybe with the exception of the fluoride lattices. In any case, the simulation of all the $4f^N$ energy levels as a whole makes it possible to observe this kind of possibilities.

3.2. *The ground term structure of Eu^{2+} and Eu^{3+}: an analytical tool?*

One should return back from the UV range down to the ground term of the R^{3+} ion, with energies up to some thousand wave numbers only. The trivalent R^{3+} ions behave usually—in their inorganic compounds, at least—as simple Curie–Weiss paramagnets at very low temperatures, let us say down to 50 K [14]. The deviations from the Curie–Weiss behavior below this temperature range are mainly due to the unequal population of the c.f. levels of the ground level (or

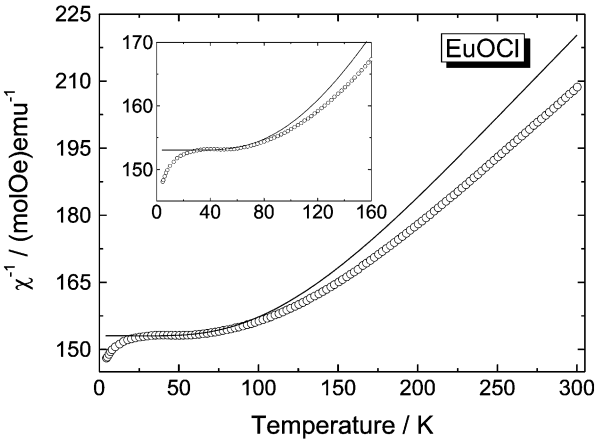

Fig. 4. Experimental (points) and calculated (solid line) paramagnetic susceptibility of europium oxychloride, EuOCl, as a function of temperature.

term) [15,16] if the coupling leading to ferro-, antiferro- and ferrimagnetisms is omitted. The deviations due to the c.f. effects can nowadays be simulated with wave functions obtained from the energy level simulations. A special case among the R^{3+} ions is the Eu^{3+} ion which shows even more different behavior from that of the other R^{3+} ions: Eu^{3+} is the best example of a strong c.f. effect on the paramagnetic susceptibility. The temperature dependence of the inverse magnetic susceptibility of Eu^{3+} (Fig. 4) is usually complex: characteristic to a Curie–Weiss paramagnet at high temperatures and then practically constant in the lower temperature range between, e.g., 75 and 25 K (for EuOCl). Finally, a sharp decrease is sometimes observed below the constant paramagnetic susceptibility range.

The temperature range where the constant paramagnetic susceptibility occurs can be explained by the exceptional ^7F_J $(J=0-6)$ ground term energy level scheme of the Eu^{3+} ion. The $^7F_0$ ground level is non-magnetic and provides no direct contribution to the paramagnetic susceptibility of Eu^{3+}. The constant paramagnetic susceptibility, which can also be called temperature independent paramagnetism (TIP), is basically due to the contributions of the magnetic levels, mainly the $^7F_2$ c.f. levels, into the wave function of the $^7F_0$ level. The amount of these contributions is controlled by the c.f. effect, especially by the B_0^2 parameter: the higher is the value of this parameter, the higher is the value of TIP. In fact, the term TIP is not entirely correct since the c.f. effect varies as a function of the temperature, decreasing with increasing temperature as a result of the expansion of the crystal lattice. The experimental verification of this very small effect, indeed, is not possible. The spin–orbit coupling introduces also some magnetic level character to the $^7F_0$ ground level mainly via mixing of the $^5D_2$ level component (through the $^5D_0$ component) but this effect is very weak due to the low contribution of these wave functions in the $^7F_0$ wave function.

As for the temperature range of the constant paramagnetic susceptibility, it also depends on the c.f. effect, in this case through the population of the excited c.f. levels, for Eu^{3+} mainly those of the $^7F_1$ level. At low temperatures, the population of these c.f. levels is close to zero but increases with temperature. Since the position of the excited c.f. levels depends on the strength of the c.f. effect, for the $^7F_1$ levels, on the value of the B_0^2 parameter, in such a way that if the crystal field is very strong (i.e., the value of the B_0^2 parameter is high), the lowest c.f. component of $^7F_1$ has a very low energy—and is populated at quite low temperatures too. Preliminary full matrix calculations have shown that a high value of the B_0^2 parameter for GdOCl:Eu^{3+} (with a C_{4v} symmetry of the R^{3+} site) leads to a short plateau of constant paramagnetic susceptibility as shown for the EuOCl in Fig. 4.

At even lower temperatures, the sharp decrease in the inverse paramagnetic susceptibility for EuOCl is due to the presence of an Eu^{2+} impurity with the $4f^7$ electron configuration. At low temperatures the Eu^{2+} ion possesses a very high paramagnetic susceptibility when compared to that of the Eu^{3+} ion. The Eu^{2+} impurity is usually present in the material because of the reduction of Eu^{3+} by the appropriate reducing agent during the preparation. The presence of the Eu^{2+} ion may be harmful in two ways: Eu^{2+} has a very strong emission due to the allowed $4f^6 5d^1 \rightarrow 4f^7$ transitions which can mask the red emission from the trivalent Eu^{3+} ion. The presence of the Eu^{2+} impurity also reduces the amount of luminescent Eu^{3+}. The usual methods to detect the valence state of europium, XPS [17] and Mössbauer [18] spectroscopies, are not sensitive enough to measure low Eu^{2+} concentrations and the EPR methods are not very well suitable for powders. Accordingly, the detection of the amount of divalent Eu^{2+} in an Eu^{3+} matrix as EuOCl is not an easy task but the measurement of the paramagnetic susceptibility of the material at low temperatures gives an indication of the Eu^{2+} ion. The determination of the Eu^{2+} content is also quantitative because of the deconvolution of the measured paramagnetic susceptibility curve into two contributions due to the Eu^{2+} and Eu^{3+} ions. The actual process is very simple: one can calculate the amount of Eu^{2+} by fitting the experimental susceptibility curve to the calculated susceptibilities of the Eu^{3+} and Eu^{2+} ions weighted by their concentrations, i.e., $\chi_{(\mathrm{exp})}=(1-a)\chi_{\mathrm{Eu(III)}}+a\chi_{\mathrm{Eu(II)}}$—or similarly with the inverse paramagnetic susceptibility. The task is facilitated by the fact that $\chi_{\mathrm{Eu(II)}}$ is behaving as a simple paramagnet to temperatures well below 4.2 K which is beyond the usually exploitable temperature range. In fact, the calculated (or experimental) paramagnetic susceptibility curve of the Gd^{3+} ion (with the same $4f^7$ electron configuration as

Eu^{2+}) in any matrix as a function of temperature can be used in the calculations. In practice, the problem is reduced to measure the paramagnetic susceptibility of the Eu^{3+} ion in the given compound since the deviation from the constant paramagnetic susceptibility is due to Eu^{2+} only. In EuOCl, the Eu^{2+} concentration was found with the use of the paramagnetic susceptibility method to be relatively low, ca. 150 ppm but still not noticed by the Mössbauer measurements [18].

4. Conclusions

The purpose of this paper was to show how useful, or even indispensable is the simulation of the energy level schemes of R^{3+} ions. Especially in the UV/VUV range, inaccessible without very expensive synchrotron measurements, the calculated energy level schemes have made it possible to predict or to prove the new phenomena as quantum cutting. On the other hand, the wave functions of the energy levels calculated as a side product in energy level simulation can be used in the calculation of a multitude of other properties of R^{3+} ions. One can mention the calculation of the g values to predict the EPR spectra, the evolution of the paramagnetic susceptibility and heat capacity as a function of the temperature and the Zeeman effect as a function of the external magnetic field as well as the calculation of the intensities of the magnetic dipole transitions. For a more experimental manner, also the energy level schemes are needed when energy transfer between unlike rare earth ions is to be required. These are not, however, treated in this paper.

Acknowledgments

Financial support from the Academy of Finland (project #204546) is gratefully acknowledged. The authors are indebted to Dr. P. Porcher for the use of the computer programs to calculate the energy level schemes as well as the magnetic properties of the $4f^N$ electron configurations. The authors want to thank Ms. A. Hietikko for collecting most of the data concerning the c.f. splittings of the $^7F_{0-4}$ levels for the Eu^{3+}-doped compounds. Most of all, we thank Dr. Carnall whose works have guided us and enabled us to carry out our work.

References

[1] G.H. Dieke, Spectra and Energy Levels of Rare Earth Ions in Crystals, Wiley Interscience, New York, 1968.
[2] S. Hüfner, Optical Spectra of Transparent Rare Earth Compounds, Academic Press, London, UK, 1978.
[3] G. Blasse, B.C. Grabmaier, Luminescent Materials, Springer, Berlin, 1994.
[4] B.G. Wybourne, Spectroscopic Properties of Rare Earths, Wiley Interscience, New York, 1965.
[5] J. Mulak, Z. Gajek (Eds.), The Effective Crystal Field Potential, Elsevier, Amsterdam, 2000.
[6] Y. Murayama, Luminous paints, in: S. Shionoya, W.M. Yen (Eds.), Phosphor Handbook, CRC Press, Boca Raton, FL, USA, 1999, p. 651.
[7] W.T. Carnall, Anal. Chem. 34 (1962) 786.
[8] W.T. Carnall, G.L. Goodman, K. Rajnak, R.S. Rana, J. Chem. Phys. 90 (1989) 3443.
[9] Y.Y. Yeung, D.J. Newman, J. Chem. Phys. 86 (1987) 6717.
[10] M.F. Reid, J. Chem. Phys. 87 (1987) 2875.
[11] C. Görller-Walrand, K. Binnemans, in: K.A. Gschneidner Jr., L. Eyring (Eds.), Handbook on the Physics and Chemistry of Rare Earths, vol. 23, North-Holland, Amsterdam, 1996, pp. 121–283.
[12] R.T. Wegh, H. Donker, A. Meijerink, R.-J. Lamminmäki, J. Hölsä, Phys. Rev. B 56 (1997) 13841.
[13] R.T. Wegh, H. Donker, E.V.D. van Loef, K.D. Oskam, A. Meijerink, J. Lumin. 87-9 (2000) 1017.
[14] J. Hölsä, M. Lastusaari, J. Niittykoski, R. Sàez Puche, Phys. Chem. Chem. Phys. 4 (2002) 3091.
[15] S. Skanthakumar, L. Soderholm, R. Movshovich, J. Alloys Comp. 303–304 (2000) 298.
[16] F. Wiss, N.P. Raju, A.S. Wills, J.E. Greedan, Int. J. Inorg. Mater. 2 (2000) 53.
[17] W. Burian, J. Szade, T. O'Keevan, Z. Celiński, Phys. Status Solidi b 241 (2004) R15.
[18] T. Aitasalo, J. Hölsä, M. Lastusaari, J. Legendziewicz, L. Lehto, J. Lindén, M. Maryško, J. Alloys Comp. 380 (2004) 296.